

Hierarchical Nanostructure Control in Rod–Coil Block Copolymers with Magnetic Fields

Yuefei Tao, Hagar Zohar, Bradley D. Olsen, and Rachel A. Segalman*

*University of California, Berkeley and Materials Science Division,
Lawrence Berkeley Laboratory, Berkeley, California 94720*

Received May 24, 2007; Revised Manuscript Received July 17, 2007

ABSTRACT

Magnetic field alignment of rod–coil block copolymers is shown to proceed through coupling to the diamagnetic moment of individual rod blocks. Block copolymer self-assembly then leads to alignment of the interfaces perpendicular to the field lines and long range order on a 10 nm lengthscale. This is in contrast to previously demonstrated alignment techniques, which couple to the block copolymer interfaces rather than individual molecules. Furthermore, alignment occurs without direct physical contact to samples millimeters in size.

Ordered block copolymer thin films are of interest in applications requiring 10 nm lengthscale patterns ranging from nanolithography to organic optoelectronics.¹ For example, the uniformly sized and shaped 10 nm domains formed in the films have been used for nanolithography, nanoparticle synthesis, and high-density information storage media while the ability to control nanometer scale internal interfaces is of vital importance to organic photovoltaics. Detailed control over nanostructure orientation and position is necessary, and surface,² electric,^{3–6} and shear fields^{7,8} have been suggested. These techniques all operate on the 10–100 nm lengthscale of block copolymer self-assembly rather than single molecules. When block copolymers are exposed to large electric fields, entire block copolymer interfaces rearrange to align parallel to the field direction.^{9,10} The field strengths necessary are very high, on order ~ 30 kV/cm,^{3–6} approaching the dielectric breakdown strengths of some polymers. Shear alignment relies on the movement of slip planes within the larger grain structure of block copolymer nanodomains.^{7,8} Both heteroepitaxy and graphoepitaxy have been used to gain positional order of cylindrical and spherical domains.¹ Each of the above alignment techniques requires special sample geometries and surface preparation in the form of electrodes, patterned surfaces, or direct contact with the surfaces of the sample in the case of shear. Ideally, templating of polymer order would occur benignly without direct, physical contact to the sample so that samples of arbitrary geometry or on arbitrary substrates may be aligned.

Magnetic fields are ideal for block copolymer structure control in that they may be applied without direct physical

contact to the sample and even high magnetic field strengths are not damaging to polymers. The directors of small molecule and polymeric liquid crystalline nematics and cholesterics are routinely aligned in magnetic fields, but alignment of smectics generally requires prohibitively large fields.¹¹ Magnetic field induced alignment of classical coil–coil block copolymers has not been demonstrated, presumably due to a lack of anisotropic magnetic susceptibility of the nanostructures. If the block copolymer contains one crystallizable block, a strong magnetic field can orient an entire crystal during crystallization resulting in a lamellar stack with the layers parallel to the magnetic field¹² (a similar geometry to that resulting from alignment in an electric field). By contrast, the incorporation of diamagnetic liquid crystalline side chains on the backbone allows direct coupling of the field to the mesogens. The flexibility of the tether between the mesogens and the backbones allows the mesogens to align somewhat independently from the backbone. Although the mesogens are aligned parallel to the field direction, the block copolymer interfaces may adopt several different orientations^{13,14} resulting in a possible lack of long range order on the block copolymer lengthscale due to degeneracies in the geometry.^{13–15}

The incorporation of a liquid crystalline main chain into the block copolymer introduces diamagnetism on a molecular level in an assembly with higher symmetry than that discussed above. Furthermore, block copolymers in which one block has a liquid crystalline, rigid shape (rod–coil block copolymers) are of particular interest since chain rigidity is frequently imparted by biological functionality (in the case of polypeptides) or π -conjugation (in the case of semiconducting block copolymers). Control over block copolymer

* Author to whom correspondence should be addressed. E-mail: segalman@berkeley.edu.

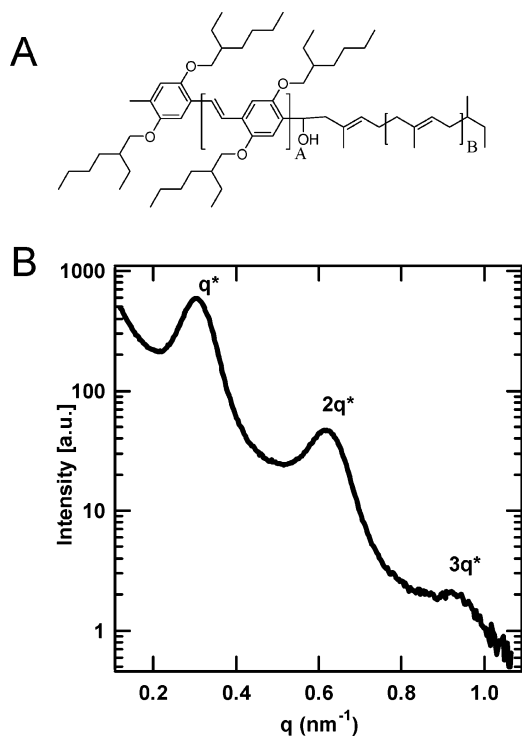


Figure 1. (A) Chemical structure of the model rod-coil block copolymer with accessible phase transitions and (B) its long range order in the lamellar phase as demonstrated by SAXS.

self-assembly is particularly important in the case of semiconducting polymers where the nanostructure is crucial in optimizing charge separation and recombination.¹⁶ We demonstrate that main-chain liquid crystalline block copolymers can be ordered in magnetic fields to not only control chain orientation on the 1 nm liquid crystalline lengthscale but also induce long range order on the 10 nm block copolymer lengthscale. The high degree of orientational control relies on the molecular anisotropy of individual rod blocks, which align parallel to the field. This molecular scale order translates into 10 nm lengthscale pattern control as the block copolymer interfaces are forced to run perpendicular to the rod direction resulting in a lamellar interface perpendicular to the field. This is in contrast to field-induced alignment of classical block copolymers where orientation relies on coupling to entire nanodomains (rather than molecular features) and results in alignment of the lamellar interface parallel to the field direction.^{3–6,12}

While the phase diagram of a bulk coil-coil block copolymer is parametrized primarily by the volume fraction of one block, the Flory-Huggins interaction parameter, and the total length of the chain, additional complexities exist in rod-coil systems due to liquid crystalline rod-rod interactions and the geometric mismatch between the rod and the coil resulting in a greatly stabilized lamellar phase.^{17–21} Model weakly segregated rod-coil block copolymers, poly-(2,5-di(2'-ethylhexyloxy)-1,4-phenylenevinylene-*block*-1,4-isoprene) (PPV-*b*-PI), shown in Figure 1, were synthesized as previously described to yield a polymer with a total molecular weight of 10 500 g/mol, polydispersity index of 1.09, and a coil volume fraction of 70%.^{17,20} The phase transitions of this polymer have been previously established

via X-ray scattering, depolarized light scattering, and polarized optical microscopy.²⁰ At temperatures greater than 130 °C, the structure is entirely isotropic. A nematic window exists between 90 and 130 °C, and the polymer forms lamellar structures with the rod oriented perpendicular to the block copolymer interface (smectic A like) below 90 °C. These lamellar structures have greater long range order in the direction perpendicular to the layer than liquid crystalline smectics, as shown in Figure 1B. At 60 °C, the PPV rods quickly crystallize into a unit cell containing two entire rods. As a result, samples may be aligned at high temperature and then quenched below 60 °C to trap order.²²

Bulk samples were sandwiched between Kapton sheets and placed in a He-purged heat stage within a 9.4 T magnetic field for alignment. Samples were then quenched to room temperature, and alignment was studied ex situ by small-angle and wide-angle X-ray scattering (SAXS and WAXS). SAXS and WAXS experiments were performed on beamline 1-4 of the Stanford Synchrotron Radiation Laboratory (SSRL). The beamline was configured with an X-ray wavelength of 1.488 Å and focused to a spot size of approximately 0.5 mm diameter. The arrangements of the B-field axis and the X-ray sample geometry are shown in Figure 2. Samples were then prepared for transmission electron microscopy (TEM) experiments by cross-linking the polyisoprene nanodomain using sulfur monochloride (S₂Cl₂) to improve mechanical stability.^{23,24} Cross-linking with S₂Cl₂ preserves the qualitative attributes of the structure but tends to swell the lamellae by approximately 30%. Thin microtomed sections (50 nm) were exposed to RuO₄ vapor to stain the poly(phenylenevinylene) nanodomains dark. TEM imaging was performed on an FEI Tecnai G2 20 TEM at 200 kV with a LaB6 filament and S-TWIN objective lens. Image shown was Fourier filtered to enhance contrast.

When aligned within the magnetic field, the liquid crystalline rod director reorients so that it is parallel to the magnetic field, as demonstrated by the radially broad peaks at 6.3 nm⁻¹ corresponding to a reflection from the 110 plane of the rods in the WAXS patterns of Figure 2. Since the block copolymer interface is confined to be perpendicular to the rod axis in our smectic A like structure, the two sharp first-order peaks in the two-dimensional (2D) SAXS at $q = 0.3 \text{ nm}^{-1}$ are perpendicular to the WAXS peaks. The radial sharpness of these peaks indicates the long range order and uniform orientation of the block copolymer interfaces over areas larger than the 0.5 mm diameter X-ray beam spot. The sample is then rotated 90° with respect to the X-rays to probe order in the orthogonal direction (X-rays incident direction parallel to the B-field) and shown in SAXS/WAXS patterns in Figure 3. In this orientation, the lamellar normal is parallel to the X-ray incident direction, so no scattering is seen on the block copolymer lengthscale in the SAXS pattern (Figure 3C). Since the rod long axis is now parallel to the X-ray incident direction, a ring is observed in the WAXS pattern for the 110 reflection confirming that the rod lattice has no preferential orientation in this plane, as expected based on the symmetry of the system. TEM imaging shown in

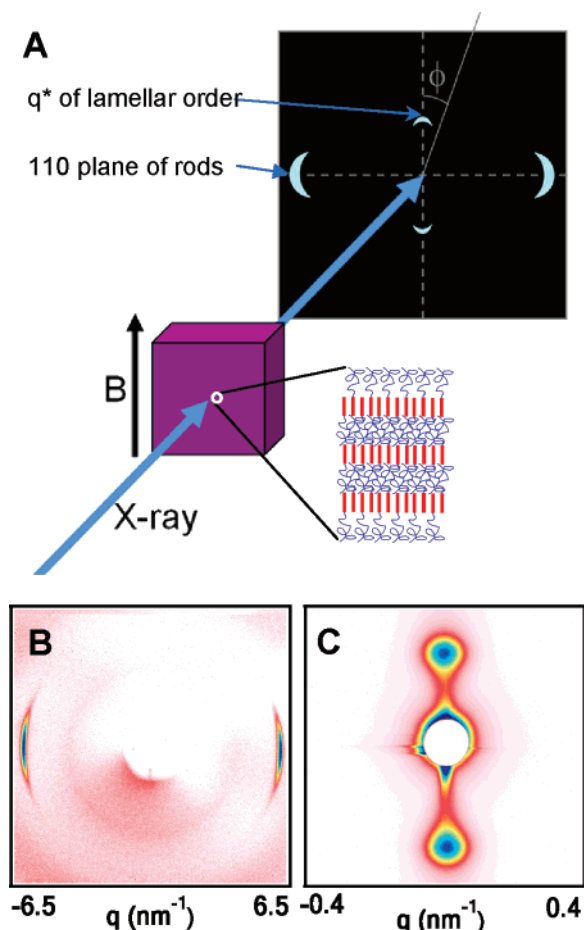


Figure 2. (A) A main chain liquid crystalline block copolymer annealed in a magnetic field at elevated temperature has its lamellar interfaces aligned. Wide-angle X-ray scattering with the X-ray incident direction perpendicular to the magnetic field direction (B) reveals that the rodlike blocks are aligned parallel to the magnetic field while small-angle X-ray scattering (C) describes the alignment of the interface perpendicular to the magnetic field direction.

Figure 4 demonstrates the high degree of detailed order on the block copolymer lengthscale. The lamellar interfaces are seen to run perpendicular to the field direction, though some waviness in lamellae is observed which may be attributed to damage during microtoming and sample preparation. In contrast to previous field alignment techniques in block copolymer pattern control, the magnetic field here couples to a liquid crystalline director on a molecular scale. Due to the high degrees of symmetry in the rod-coil block copolymer, the controlled orientation of the molecular rods translates to long range order in three dimensions on the block copolymer lengthscale. Furthermore, since the magnetic field orientation occurs on a molecular level, the orientation of nanodomains is orthogonal to the previously studied cases where the field (electric or magnetic) worked on nanodomain interfaces.^{3,4,6,12,25}

The thermal history of the sample during exposure to an aligning field strongly influences the degree of order observed. Azimuthal scans of 2D SAXS patterns taken in the geometry shown in Figure 2 clearly demonstrate the large degrees of order achieved and allow for the comparison of the effects of thermal history (Figure 5). An order parameter,

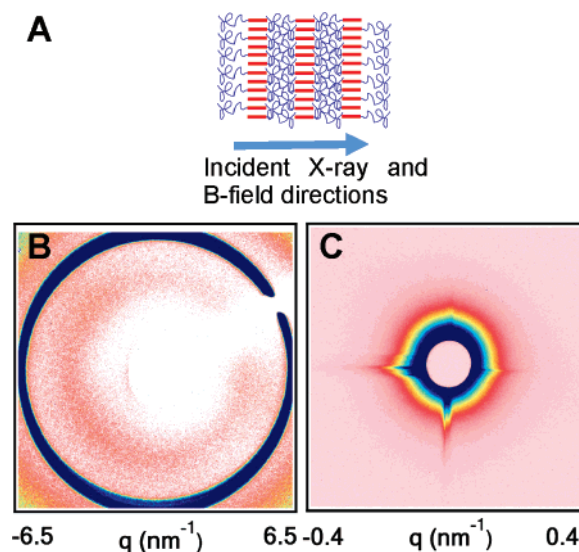


Figure 3. (A) Sample is rotated 90° within the X-ray scattering line so that the incident X-ray and B-field are parallel. (B) As expected, the long axis of the rodlike block is now parallel to the incident X-ray direction and the rods do not display preferential alignment within the layer plane as displayed by a ring at 6.3 nm⁻¹ in WAXS. (C) The lamellar interfaces are now perpendicular to the incident X-rays and do not scatter, so no peak is seen at the block copolymer lengthscale (0.3 nm⁻¹).

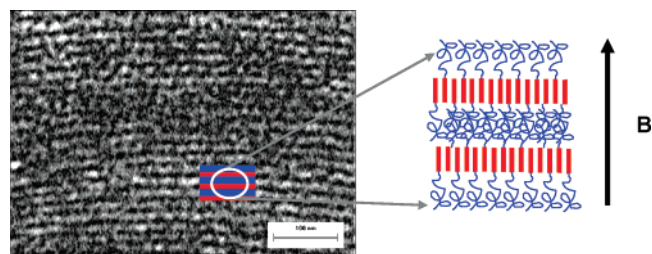


Figure 4. Transmission electron microscopy demonstrates the alignment of the block copolymer interfaces perpendicular to the magnetic field. Some waviness in the interfaces is introduced by the cross-linking and staining procedures necessary in the preparation of the microscopy sample.

P_2 , further quantifies the degree of order in the block copolymer interfaces as observed through a 2D SAXS pattern

$$\langle P_2 \rangle = \frac{3\langle \cos^2 \phi \rangle - 1}{2} \quad (1)$$

where

$$\langle \cos^2 \phi \rangle = \frac{\int_0^{2\pi} I(\phi) \cos^2 \phi |\sin \phi| d\phi}{\int_0^{2\pi} I(\phi) |\sin \phi| d\phi} \quad (2)$$

where ϕ is the azimuthal angle made between the first-order peak and the magnetic field direction as shown in Figure 2A and $I(\phi)$ is the intensity distribution of the 100 reflection along in the ϕ direction. Perfect alignment of the block copolymer lamellae in the expected direction perpendicular to the field will result in $P_2 = 1$ while no preferred

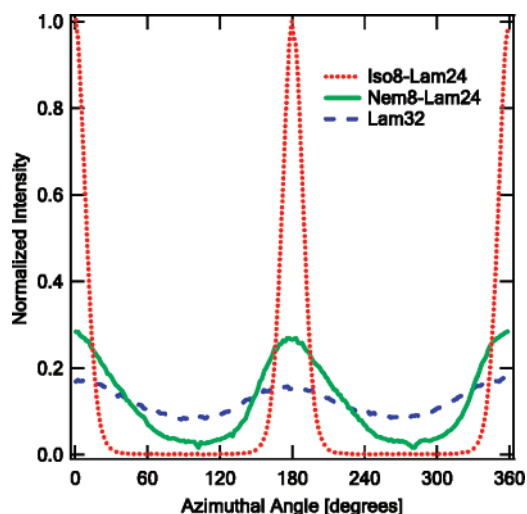


Figure 5. Intensity scans in the azimuthal direction demonstrate the highest degree of order is observed upon annealing samples first above the microphase disorder transition and then quenching into the lamellar phase to allow nanostructuring to occur. All scans have been normalized to have equal total scattering intensity. A key to sample names is included in Table 1.

orientation would yield $P_2 = 0$ and perfect order in the unexpected direction parallel to the field would have $P_2 = -0.5$.

While a sample aligned in the smectic phase is somewhat preferentially oriented ($P_2 = 0.32$), it is evident from azimuthal scans shown in Figure 5 that much better order results when the block copolymer is first exposed to the field above the temperature at which the rods and coils start to mix (microphase disordering temperature) and the free energy barrier to reorienting chains is minimal. The samples must then be further aligned in the lamellar regime so that the block copolymer texture may form. This is similar to the case of classical coil–coil block copolymers in which the best orientational control is achieved when they are sheared initially in the disordered state.²⁶

In the present case, the samples are initially in a polygrain lamellar structure at room temperature. When they are heated into the nematic phase within the magnetic field, initially a polygrain nematic texture is formed. It appears that the kinetics for removal of grain boundaries and disclinations (alignment) in the polygrain nematic to form a single domain, aligned nematic in the field is quite slow resulting in only moderate degrees of long range order. This degree of order, however, increases appreciably (P_2 values increase from 0.5 to 0.75) as a function of time spent in the nematic phase, as shown in Table 1. The best order is obtained when aligning first in the isotropic temperature range to form a single domain nematic and then cooling into the lamellar phase while still in the magnetic field ($P_2 > 0.9$). The required time within the isotropic temperature range appears to be quite small (<8 h), but a longer period of time in the lamellar phase is necessary to allow for nanostructure formation. In the isotropic phase, rod–rod attractions in the block copolymer are outweighed by the entropy produced by disorientation. Access of the isotropic phase may simply erase the thermal history (grain boundaries originating from

Table 1. Effect of Thermal History on Alignment

sample	temperature profiles during alignment within B-field	P_2
Iso8-Lam24	140 °C (8 h) → 80 °C (24 h)	0.914
Iso16-Lam16	140 °C (16 h) → 80 °C (16 h)	0.898
Iso24-Lam8	140 °C (24 h) → 80 °C (8 h)	0.844
Nem8-Lam24	115 °C (8 h) → 80 °C (24 h)	0.542
Nem16-Lam16	115 °C (16 h) → 80 °C (16 h)	0.738
Lam32	80 °C (32 h)	0.382

the sample preparation) allowing for an easier path toward an aligned lamellar upon quenching. Alternatively, when a block copolymer heated to a temperature within the isotropic range is exposed to the magnetic field, the external force may align the rods to form a single domain nematic which then eases the transition to a well-ordered lamellar phase. Differentiation between these mechanisms is the subject of ongoing experiments.

We demonstrate a new route for creating 10 nm length-scale patterns in controllable directions by incorporating a diamagnetic block copolymer. Magnetic fields couple directly to the liquid crystalline director of the rod block of a rod–coil block copolymer allowing for control over the liquid crystalline lengthscale. The inherent symmetry of the system translates this molecular scale alignment to long range order in three dimensions on the 10 nm block copolymer lengthscale, as demonstrated by SAXS, WAXS, and TEM. This suggests a new route for 10 nm lengthscale patterning which allows for arbitrary sample geometry and does not require special sample fabrication or surface damage. Control is best when the sample is first aligned at a high temperature within the isotropic range and then held in a lower temperature mobile lamellar phase to allow for reorientation.

Acknowledgment. We gratefully acknowledge support from an NSF-CAREER Award and the Department of Energy Office of Basic Energy Sciences through the Plastic Electronics Program at Lawrence Berkeley National Lab (LBNL). SAXS and WAXS experiments were performed at the Stanford Synchrotron Radiation Laboratory, a national user facility operated by Stanford University and supported by the Department of Energy, Office of Basic Energy Sciences. B.D.O. gratefully acknowledges a Hertz Foundation Fellowship and H.Z. gratefully acknowledges support from an NSF Graduate Fellowship. We thank the Pines, Reimer, and Alivisatos groups at UC Berkeley for assistance and use of some equipment (magnets and TEM) employed in this study. We also thank Edward J. Kramer and Nitash P. Balsara for helpful discussions.

References

- (1) Segalman, R. A. *Mater. Sci. Eng. R* **2005**, *48* (3), 191–226.
- (2) Kim, S. O.; Solak, H. H.; Stoykovich, M. P.; Ferrier, N. J.; de Pablo, J. J.; Nealey, P. F. *Nature* **2003**, *424* (6947), 411–414.
- (3) Xu, T.; Zhu, Y. Q.; Gido, S. P.; Russell, T. P. *Macromolecules* **2004**, *37* (7), 2625–2629.
- (4) Mansky, P.; DeRouchey, J.; Russell, T. P.; Mays, J.; Pitsikalis, M.; Morkved, T.; Jaeger, H. *Macromolecules* **1998**, *31* (13), 4399–4401.
- (5) Amundson, K.; Helfand, E.; Davis, D. D.; Quan, X.; Patel, S. S.; Smith, S. D. *Macromolecules* **1991**, *24* (24), 6546–6548.

- (6) Morkved, T. L.; Lu, M.; Urbas, A. M.; Ehrichs, E. E.; Jaeger, H. M.; Mansky, P.; Russell, T. P. *Science* **1996**, *273* (5277), 931–933.
- (7) Wu, M. W.; Register, R. A.; Chaikin, P. M. *Phys. Rev. E* **2006**, *74* (4), 040801.
- (8) Angelescu, D. E.; Waller, J. H.; Register, R. A.; Chaikin, P. M. *Adv. Mater* **2005**, *17* (15), 1878–1881.
- (9) Pereira, G. G.; Williams, D. R. M. *Macromolecules* **1999**, *32* (24), 8115–8120.
- (10) Tsori, Y.; Tournilhac, F.; Leibler, L. *Macromolecules* **2003**, *36* (15), 5873–5877.
- (11) Gennes, P. G. d.; Prost, J. *The physics of liquid crystals*, 2nd ed.; Clarendon Press, Oxford University Press: Oxford, New York, 1993; p xvi, p 597.
- (12) Grigorova, T.; Pispas, S.; Hadjichristidis, N.; Thurn-Albrecht, T. *Macromolecules* **2005**, *38* (17), 7430–7433.
- (13) Hamley, I. W.; Castelletto, V.; Lu, Z. B.; Imrie, C. T.; Itoh, T.; Al-Hussein, M. *Macromolecules* **2004**, *37* (13), 4798–4807.
- (14) Osuji, C.; Ferreira, P. J.; Mao, G. P.; Ober, C. K.; Vander Sande, J. B.; Thomas, E. L. *Macromolecules* **2004**, *37* (26), 9903–9908.
- (15) Tomikawa, N.; Lu, Z. B.; Itoh, T.; Imrie, C. T.; Adachi, M.; Tokita, M.; Watanabe, J. *Jpn. J. Appl. Phys., Part 2* **2005**, *44* (20–23), L711–L714.
- (16) Yang, X.; Loos, J. *Macromolecules* **2007**, *40* (5), 1353–1362.
- (17) Olsen, B. D.; Segalman, R. A. *Macromolecules* **2005**, *38* (24), 10127–10137.
- (18) Olsen, B. D.; Segalman, R. A. *Macromolecules* **2006**, *39* (20), 7078–7083.
- (19) Olsen, B. D.; Li, X. F.; Wang, J.; Segalman, R. A. *Macromolecules* **2007**, *40* (9), 3287–3295.
- (20) Tao, Y.; Olsen, B. D.; Ganesan, V.; Segalman, R. A. *Macromolecules* **2007**, *40* (9), 3320–3327.
- (21) Pryamitsyn, V.; Ganesan, V. *J. Chem. Phys.* **2004**, *120* (12), 5824–5838.
- (22) Olsen, B. D.; Jang, S. Y.; Luning, J. M.; Segalman, R. A. *Macromolecules* **2006**, *39* (13), 4469–4479.
- (23) Ishizu, K. J.; Onen, A. *J. Polym. Sci., Part A: Polym. Chem.* **1989**, *27* (11), 3721–3731.
- (24) Liu, G. J.; Yan, X. H.; Duncan, S. *Macromolecules* **2002**, *35* (26), 9788–9793.
- (25) Tsori, Y.; Andelman, D. *Macromolecules* **2002**, *35* (13), 5161–5170.
- (26) Koppi, K. A.; Tirrell, M.; Bates, F. S. *Phys. Rev. Lett.* **1993**, *70* (10), 1449–1452.

NL0712320